

Single-crystal nanocastles of ZnO

Xudong Wang, Jinhui Song, Zhong Lin Wang *

School of Materials Science and Engineering, Georgia Institute of Technology, Atlanta, GA 30332-0245, USA

Received 22 March 2006; in final form 5 April 2006

Available online 27 April 2006

Abstract

As a result of switching the growth from hexagonal disks to nanorods/nanobelts, single-crystalline ‘nanocastles’ of ZnO have been synthesized. This new structure was constructed by two basic parts: a sheet-like hexagonal crystal base and vertical nanorods/nanobelts surrounding the base as the ‘walls’ of the castle. Moreover, for the first time, ZnO nanorods with a triangular and diamond cross-sections were found growing on top of the nanocastles. The whole nanocastle structure was enclosed by the (0001) and $\{01\bar{1}0\}$ facets. This configuration is a new member in the family of ZnO nanostructures. The in situ morphology switching mechanism would be an useful technique for fabricating high quality heterostructures or interconnects at nanometer scale.

© 2006 Elsevier B.V. All rights reserved.

1. Introduction

Zinc oxide is one of the most important functional materials [1]. With a direct bandgap of 3.37 eV, a high electron-hole binding energy of 60 meV and non-centrosymmetric crystal structure, ZnO has been widely used as optoelectronics [2], piezoelectric devices and sensors [3]. Due to its hexagonal Wurtzite structure and polar crystal surfaces, ZnO exhibits a large family of nanostructures [4]. In addition to the conventional nanowire and nanobelt [5] structures, many interesting morphologies have been discovered recently, such as nanocages [6], nanocombs [7], nanorings [8], nanosprings [9,10], nanobows [11], and nanodisks [12,13]. Those structures not only provided valuable models in understanding crystal growth mechanisms in nanometer scale, but also exhibited high potential for fabricating novel nano electronic and optical devices with enhanced performance.

Different morphologies were generally induced by different vapor concentration. It has been found that changing the ZnO vapor concentration during the growth can switch the growth morphology from nanowire to curved nanobelts [14], thus, forming a nanobow structure. In this Let-

ter, by quickly cooling down the furnace, we have successfully switched the growth from hexagonal disks to nanorods/nanobelts, resulting in the formation of a ‘nanocastle’, a new structural configuration for ZnO. The morphology is basically composed of two parts: quasi-two-dimensional (2D) hexagonal crystal base and quasi-one-dimensional (1D) nanostructures surrounding the base as the ‘walls’ of the nanocastle. The two different structures appeared to grow consecutively and formed a single-crystal structure.

2. Experiments

The nanocastles were fabricated through a carbon-thermal evaporation process. In a typical experiment, 0.3 g of high purity ZnO powders were mixed with 0.3 g of graphite powders as the source materials and the mixture was loaded into a quartz boat. The substrate was a $5 \times 5 \text{ mm}^2$ *c*-plane orientated sapphire coated with a thin-layer of single-crystal *c*-plane GaN. A droplet of 15 nm gold colloidal solution (purchased from Ted Pella Inc.) was dispersed onto the substrate as deposition seeds and the additional solution was quickly blew away by nitrogen. In order for an ultra-high vapor concentration, a double-tube setup was used for crystal growth. In this system, the source material was put at the center of a 22-mm-wide, 30-cm-long

* Corresponding author. Fax: +1 404 894 9140.

E-mail address: zhong.wang@mse.gatech.edu (Z.L. Wang).

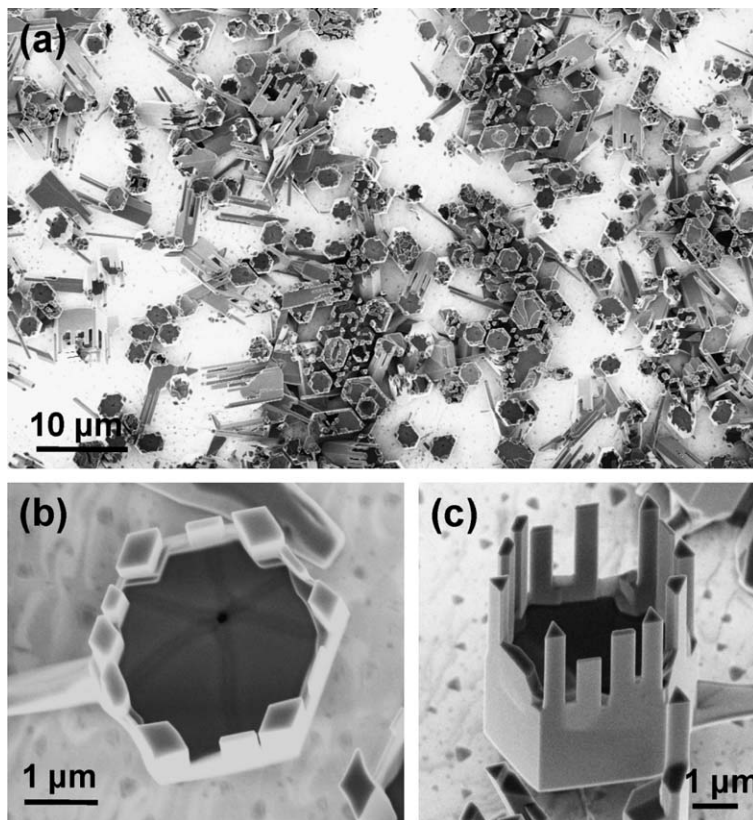


Fig. 1. (a) Low magnification SEM image of the as-synthesized nanocastles grown on GaN substrate; (b) higher magnification SEM image of the top view of a nanocastle; and (c) 30° side view of a nanocastle.

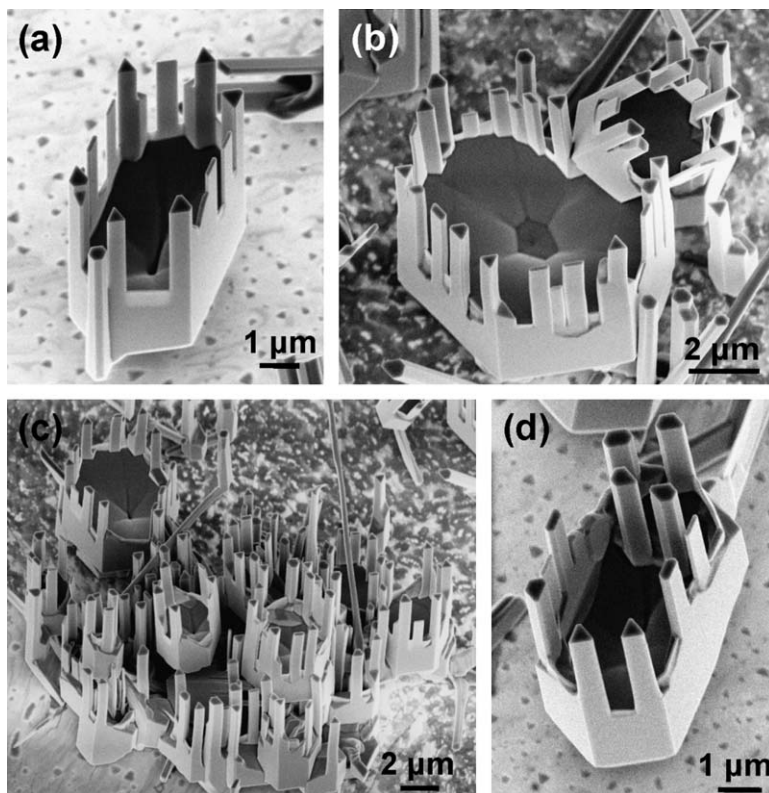


Fig. 2. SEM images of nanocastles with different morphologies. (a) An elongated hexagonal nanocastle; (b) the biggest nanocastle with a size ~ 10 μm; (c) a bundle of nanocastles growing together; and (d) a nanocastle with nanorods growing inside.

quartz tube, while the substrate was located 10 mm from the source boat. This small tube was loaded into a 36-mm-wide alumina tube in a horizontal tube furnace, where the source was retained at the center. After pumping down the tube chamber to ~ 10 mtorr, the furnace was turned on and heated to 950°C at a rate of $50^\circ\text{C}/\text{min}$. Meanwhile, high-purity Ar was introduced into the tube at a flow rate of 50 sccm to bring the chamber pressure back to 150 torr. The temperature and pressure were held for 30 min. Then the furnace was turned off and the system was quickly cooled down below 500°C within 10 min with the help of a fan. The deposited structure was characterized by LEO 1530 field emission scanning electron microscopy (SEM) and Hitachi HF2000 transmission electron microscopy (TEM).

3. Results and discussion

3.1. Morphologies of the nanocastles

The as-synthesized products were first examined by SEM. Fig. 1a is a low magnification SEM image showing the scattered distribution of the nanocastles owing to the low concentration of the gold nanoparticle solution. Dictated by the sixfold symmetry of the Wurtzite ZnO crystal, all of the nanocastles exhibited a hexagonal-like shape. The perfect lattice match between GaN and ZnO made most of the nanocastles orientated perpendicular to the substrate. The size of the nanocastle varied from $2\ \mu\text{m}$ to $10\ \mu\text{m}$, while the majority is $\sim 3\ \mu\text{m}$. A typical nanocastle is shown in a higher resolution SEM image in Fig. 1b. On the hexagonal ZnO base, six diamond-shaped nanorods grew at the six corners of the hexagon. Between every two nanorods, there are six nanobelts with a thickness of ~ 50 nm and a width of ~ 500 nm growing along the six flat surfaces. The castle-like morphology can be more clearly presented by a side-view SEM image, as shown in Fig. 1c. The thickness of the ZnO base is $\sim 2\ \mu\text{m}$ and the lengths of the top nanobelts/nanorods are $3\sim 4\ \mu\text{m}$. The nanobelts/nanorods and the ZnO base share a smooth outer surface and no trace of connection could be observed at the junctions. However, unlike the nanocastle shown in Fig. 1b, the corner posts of this one have a triangular cross-section.

When the size of nanocastles was bigger than $3\ \mu\text{m}$, they were more likely to be elongated hexagons, as shown in Fig. 2a. Six triangular posts only grew at the corners. On the longer side, more nanobelts can be grown along the edge, while their widths were still remained at ~ 500 nm. The biggest nanocastle was found to be $\sim 10\ \mu\text{m}$, as shown in Fig. 2b. Its corner-rods and side-belts configuration was identical to the smaller ones, however, their large side surfaces allowed more nanobelts to grow.

Multiple nanocastles could grow together side-by-side or overlapping with each other constructing a multi-level larger castle, as shown in Fig. 2c. Nanorods and nanobelts grew around the edges that were not covered by the others. All of them exhibited similar length and width/thickness

regardless the size of their bases. In some cases, a few nanorods can also grow inside the nanocastle, as shown in Fig. 2d. It's possibly because additional nucleation sites were created on the base surface during the growth. The nanorods in the center showed a conventional hexagonal cross-section since there was no restriction from the pre-existed side surfaces, which would change the growth rates of the six equivalent side facets.

3.2. Structure characterization

TEM analyses were performed to characterize the crystal structure of the nanocastles. Fig. 3a shows a typical low-magnification TEM image of a nanocastle. Although some nanorods/nanobelts were broken due to sample preparation, the configuration of the nanocastle can be clearly distinguished. The nanobelts showed a light contrast with bending contours, while the contrast of the nanorods was much darker due to their larger thickness. Fig. 3b shows a closer view of the nanobelts structure inside the rectangular box in Fig. 3a. The uniform contrast indicates the uni-

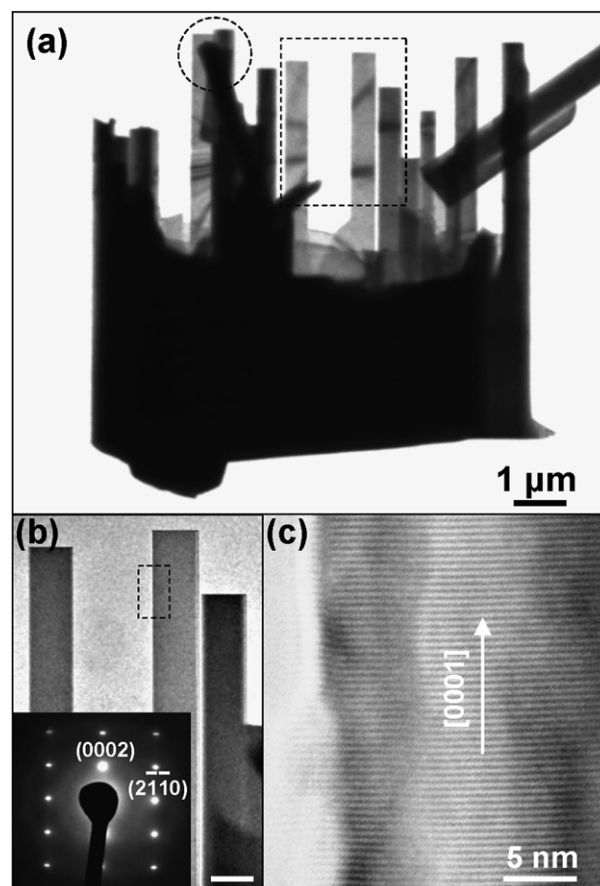


Fig. 3. (a) A low magnification TEM image of a nanocastle. (b) An enlarged nanobelt structure inside the rectangular box of Fig. 3a; the scale bar represent 500 nm. Inset: a corresponding electron diffraction pattern recorded on the nanobelt. (c) A high resolution TEM image showing the ZnO lattice recorded on the nanobelt area inside the rectangular box of Fig. 3b.

form thickness along the whole nanobelt. A corresponding diffraction pattern reveals that the nanobelt was growing along the $[0001]$ direction and its top and side surfaces were $(01\bar{1}0)$ and $(2\bar{1}\bar{1}0)$ surfaces, respectively, as shown in the inset of Fig. 3b. The ZnO single-crystal lattice is shown by a high-resolution TEM image (Fig. 3c) recorded at the edge of the nanobelt indicated by a rectangular box in Fig. 3b.

Conventionally, the cross-section of ZnO nanowires was hexagonal. For the first time, triangular-shaped ZnO nanowires were synthesized, although the triangular morphology has already been found for GaN nanowires [15]. The nanorod circled in Fig. 3a has a triangular cross-section. By tilting the sample, the flat triangular tip can be clearly observed, as shown in Fig. 4a. In order to reveal its surface configuration, one surface of the nanorod was tilted to be perpendicular to the incident electron beam, as shown in Fig. 4b. The corresponding diffraction pattern is shown in Fig. 4c, which is the same as the one taken from the nanobelt. Thus, the side surfaces of the triangular nanorod can be identified as three $\{01\bar{1}0\}$ facets and they are 60° from each other, as shown in Fig. 4d. Select-area electron diffraction pattern was also recorded on the thin area of the base crystal and an exactly same pattern was acquired. This confirms that the entire nanocastle was formed by a single crystal piece of ZnO.

Therefore, in general, the nanocastle was composed by the six equivalent $\{01\bar{1}0\}$ facets and its growth direction is along the $[0001]$. Accordingly, the nanobelts and nanorods shared the same group of outer facets, as illustrated by

Fig. 4e. The nanobelts only grew along the edges, where only one surface could be supported. Diamond and triangular nanorods only grew at corners, where two surfaces were confined. From their orientations and angles between their facets, it could be concluded that the triangular nanorods are exactly one half of the diamond nanorods. The formation of the triangular nanorods is likely due to space restriction when the space at one side was taken by a neighboring nanobelt. Nothing would grow at the corner if the nanobelts on both sides grew too close. Nevertheless, the nanobelts, diamond and triangular nanorods were composed by the same group of $\{01\bar{1}0\}$ facets and these three different morphologies could be found on the same nanocastle, as shown in Fig. 4d.

3.3. Growth mechanism

In accordance with the SEM and TEM characterization, a possible growth mechanism of the nanocastles was proposed as illustrated in Fig. 5a. Catalyzed by a gold nanoparticle, a small piece of ZnO nanocrystal was first deposited. Due to the very high ZnO vapor concentration, the lateral growth along six $\langle 2\bar{1}\bar{1}0 \rangle$ directions became much faster. Moreover, the edge areas were much more active than the center. After a period of time, a hexagonal plate was formed with an increasing thickness from center to edges.

When the furnace was turned off, the vapor concentration quickly dropped down and the lateral growth became no longer favorable. However, the vapor concentration

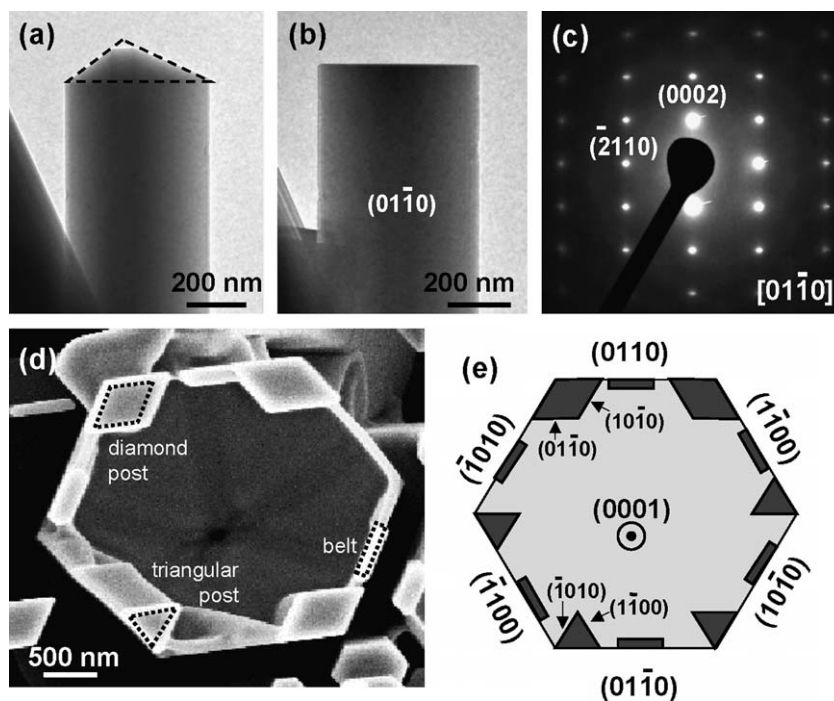


Fig. 4. (a) A TEM image of a triangular nanorod grown on the nanocastle shown in the circled area in Fig. 3a; (b) a TEM image of the same triangular nanorod that has been tilted perpendicular to the incident electron beam; (c) a corresponding diffraction pattern recorded on the nanorod; (d) a top view SEM image of a nanocastle that has nanobelt, triangular nanorod and diamond nanorod growing together; and (e) a schematic of the crystal configuration of a nanocastle.

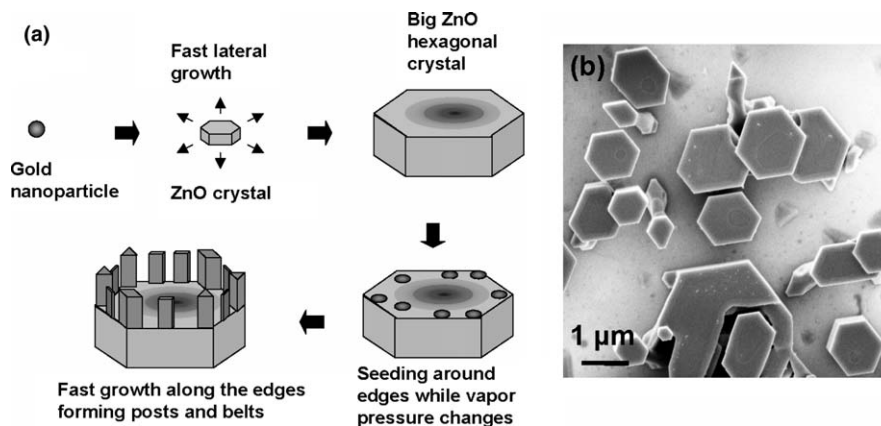


Fig. 5. (a) Schematic steps of the formation of nanocastles and (b) a SEM image of hexagonal ZnO base crystals that were held at the second nucleation stage.

may still over the supersaturation level and new nucleus would be induced around the edge of the large ZnO plate. The low supersaturation level was preferred by linear growth. Consequently, 1D nanostructures were grown out along the edges, which were the most active area due to higher percentage of dangling bonds. Since the incoming source vapor was limited after turning off the furnace, most of the vapor was consumed in the front area of the substrate to form nanocastles and the vapor concentration couldn't reach the supersaturation level on the downstream side. As a result, the ZnO plates were left at the second nucleation stage. Fig. 5b shows the platelet structure acquired at the down-stream side, which shows the hexagonal ZnO plates with tiny nucleus. This is direct evidence supporting our growth mechanism.

The mechanism could be a general route of the in situ morphology switching, which is induced by the vapor concentration change inside the growth chamber. As long as the desired vapor concentration is identified for different morphologies, such as nanobelts, nanorods, nanodisks, or nanotubes, the nanostructures would be switched during the growth once their desired growth condition is reached. This is a technique beyond simple morphology control and achieves different morphologies growing together with a control sequence.

4. Conclusion

In this Letter, a new nanocastle morphology was found for the family of ZnO nanostructures. It is formed by two different basic structures: a 2D hexagonal crystal base and 1D nanorods/nanobelts surrounding the base as the 'walls' of the castle. These two different structures seamlessly grew together and formed a single-crystal. The switching of morphology was induced by changing the vapor concentration during the growth. Moreover, ZnO nanorods were first found with a triangular and diamond cross-section owing to the surface confinement from the bottom ZnO base.

The whole nanocastle structure was grown along the [0001] direction and surrounded by the six equivalent $\{01\bar{1}0\}$ facets. The synthesis of this new nanocastle morphology could enrich our knowledge about Wurtzite crystal growth, and it presents a new structural configuration with potential applications. The in situ morphology switching mechanism presented in this Letter would be an useful technique for fabricating high quality heterostructures or interconnects at nanometer scale.

Acknowledgement

Thanks to support from NSF, the NASA Vehicle Systems Program and Department of Defense Research and Engineering (DDR&E), and the Defense Advanced Research Projects Agency.

References

- [1] Ü. Özgür, Y.I. Alivov, C. Liu, A. Teke, M.A. Reshchikov, S. Doğan, V. Avrutin, S.-J. Cho, H. Morkoç, *J. Appl. Phys.* 98 (2005) 041301.
- [2] M. Huang, S. Mao, H. Feick, H. Yan, Y. Wu, H. Kind, E. Weber, R. Russo, P. Yang, *Science* 292 (2001) 1897.
- [3] C. Yu, Q. Hao, S. Saha, L. Shi, X. Yang, Z.L. Wang, *Appl. Phys. Lett.* 86 (2005) 063101.
- [4] Z.L. Wang, *Mater. Today* 7 (2004) 26.
- [5] Z.W. Pan, Z.R. Dai, Z.L. Wang, *Science* 291 (2001) 1947.
- [6] P.X. Gao, Z.L. Wang, *J. Am. Chem. Soc.* 125 (2003) 11299.
- [7] Z.L. Wang, X.Y. Kong, J.M. Zuo, *Phys. Rev. Lett.* 91 (2003) 185502.
- [8] X.Y. Kong, D. Yong, R. Yang, Z.L. Wang, *Science* 303 (2004) 1348.
- [9] X.Y. Kong, Z.L. Wang, *Nanoletter* 3 (2003) 1625.
- [10] P.X. Gao, Y. Ding, W. Mai, W.L. Hughes, C.S. Lao, Z.L. Wang, *Science* 309 (2005) 1700.
- [11] W.L. Hughes, Z.L. Wang, *J. Am. Chem. Soc.* 126 (2004) 6703.
- [12] P.X. Gao, C.S. Lao, D. Yong, Z.L. Wang, *Adv. Funct. Mater.* 16 (2006) 53.
- [13] F. Li, Y. Ding, P. Gao, X. Xin, Z.L. Wang, *Angew. Chem.* 116 (2004) 5350.
- [14] W.L. Hughes, Z.L. Wang, *Appl. Phys. Lett.* 86 (2005) 043106.
- [15] F. Qian, Y. Li, S. Gradecak, D. Wang, C.J. Barrelet, C.M. Lieber, *Nanoletter* 4 (2004) 1975.